Biocybernetics and Biomedical Engineering 46 (2026) 608–618

Contents lists available at ScienceDirect

Biocybernetics and Biomedical Engineering

journal homepage: www.elsevier.com/locate/bbe

Research Paper

A framework based on information dynamics to assess and dissect complex cardiovascular interactions across pathophysiological states

Stefano Cimignolo [a,*], Chiara Barà [b,c], Riccardo Pernice [b], Luca Faes [b], Giandomenico Nollo [a], Michela Masè [a]

[a] Department of Industrial Engineering, University of Trento, Trento, 38123, Italy
[b] Department of Engineering, University of Palermo, Palermo, 90128, Italy
[c] National Research Council, Institute of Intelligent Technologies and Systems for Advanced Manufacturing, Milano, 20133, Italy

ARTICLE INFO

Keywords:
Cardiovascular dynamics
Information decomposition
Causality
Physiological time series analysis
Cardiovascular disease

ABSTRACT

The assessment of cardiovascular dynamics from heart period (RR) and systolic arterial pressure (SAP) time series requires analytical tools capable of capturing the complexity and nonlinearity of the underlying regulatory mechanisms and the directionality of their interactions. This work presented and tested a methodological framework combining Mutual Information Rate (MIR) with multiple surrogate data analysis to quantify and statistically validate complexity, causality, and nonlinearity in cardiovascular dynamics. Specifically, MIR was estimated through a model-free nearest-neighbor approach and decomposed into measures of complexity (i.e., entropy rate) and causality (i.e., transfer entropy). The capability of the method to characterize cardiovascular regulation was evaluated across young normotensive healthy subjects, older healthy individuals, and post-acute myocardial infarction (AMI) patients, undergoing an orthostatic stress test. In healthy young subjects, orthostatic stress induced the expected reduction in cardiovascular entropy rate and nonlinear coupling, reflecting a regulated baroreflex response. In contrast, older adults and post-AMI patients exhibited altered dynamics already at rest and lacked the adaptive modulation observed in the young group. These results demonstrated the potential of MIR decomposition, supported by surrogate analysis, as a robust framework to characterize the modulation of cardiovascular control mechanisms in response to orthostatic stress and their alterations across pathophysiological conditions.

1. Introduction

Cardiovascular diseases involve pathological alterations of the heart and blood vessels and are responsible for 32% of global deaths according to the World Health Organization [1]. The assessment of cardiovascular dynamics is thus crucial for early diagnosis of pathological states and the application of targeted treatments, both pharmacological and clinical [2]. The primary function of the cardiovascular system is to ensure adequate blood perfusion and, consequently, enable the transportation of oxygen and nutrients to all body tissues through the combined action of the heart and the vascular network [3]. The maintenance of cardiovascular homeostasis, particularly in response to physiological or stress-inducing stimuli, is the result of the complex integration of a multiplicity of mechanisms and feedback pathways, including respiratory, baroreflex, and chemoreflex interactions, acting at both central and peripheral levels [4–9]. The resulting temporal fluctuations in cardiac and pressure signals thus reflect the coordinated activity of these coupled control mechanisms [10,11]. The autonomic nervous system (ANS) plays a key role in coordinating cardiovascular regulation through the interaction of its sympathetic and parasympathetic activity [12–14]. By modulating heart rate and vascular resistance, the ANS contributes to the control of arterial pressure, which is continuously stabilised through the baroreflex mechanism. The baroreflex system constitutes a closed-loop feedback circuit essential for the beat-to-beat regulation of systolic arterial pressure (SAP) and heart period (RR interval from the ECG). It operates through the activity of baroreceptors, central nervous system integration centers, and sympathetic and vagal efferent pathways [15–17]. Under physiological conditions, such as during orthostatic stress, these mechanisms enable the stabilization of arterial pressure and ensure adequate cerebral perfusion. The baroreflex exerts bidirectional control, where SAP influences heart rate via a negative feedback mechanism, and heart rate influences SAP in a feedforward manner, through mechanical pathways and modulation of venous return and cardiac output (CO) [17–19]. These regulatory mechanisms and their interactions

* Corresponding author.
E-mail address: stefano.cimignolo@unitn.it (S. Cimignolo).

https://doi.org/10.1016/j.bbe.2026.07.003
Received 27 November 2025; Received in revised form 23 July 2026; Accepted 24 July 2026
Available online 11 August 2026

produce complex and nonlinear dynamics, which can be indirectly observed and characterized from the resulting RR interval and SAP time series. The dynamics are sensitive to increasing age or pathological conditions that may compromise the effectiveness of autonomic control [20–22]. A thorough description of such dynamics requires the use of advanced analytical methods capable of capturing both the nonlinear nature and the directionality of the interactions between SAP and RR [23].

In this context, several approaches have been proposed to describe and model physiological regulation at the system level. In particular, the fields of network physiology and computational physiology have been introduced to interpret physiological signals as the result of interacting subsystems and to provide quantitative models of their underlying mechanisms [11,24,25].

In line with this approaches, cardiovascular regulation has been characterized in many studies using univariate analyses of heart rate or arterial pressure variability, mainly through entropy-based indices or standard Heart Rate Variability (HRV) metrics [26,27]. These approaches describe the variability of individual signals, but they do not capture the bidirectional closed-loop interaction between SAP and RR. To include directionality, linear bivariate models, such as Granger causality and spectral baroreflex estimates, have been applied to quantify feedforward and feedback components of SAP-RR coupling [28–31]. However, as shown in recent works [10,22,32], linear causality metrics detect only global linear coupling and fail to identify nonlinear adaptive dynamics, which are relevant for physiological regulation under stress or pathological conditions. In response to these limitations, information-theoretic measures have emerged as powerful alternatives [32–34]. Among these measures, Mutual Information Rate (MIR) [35], a measure of the stochastic interaction between two random processes [36,37], has gained significant popularity in bivariate time series analysis due to its decomposability into measures providing insights on both the uncertainty (closely related to complexity) and causality of the series [33,38–40]. Moreover, the use of nonparametric approaches for estimating MIR, such as the approach based on k-nearest neighbors (KNN), allows to account for the nonlinear nature of the investigated dynamics. However, given the inherent variability and stochastic nature of physiological processes, complexity, causality, and nonlinearity aspects need to be statistically-validated to assess their reliability. In this context, surrogate data analysis provides a rigorous statistical framework to assess the significance of MIR and its decomposition terms, and to discriminate whether the observed interactions reflect nonlinear dynamics [32,34,41].

Based on these concepts, this study proposes a comprehensive framework of analysis, which relies on the combination of MIR and its decomposition with a statistical approach based on multiple surrogate data generation. The capability of the proposed framework to provide a thorough quantification of cardiovascular interactions, in terms of entropy rate, causality, and nonlinearity, was evaluated by application to RR interval and SAP time series, which provides a representative bivariate projection of the underlying cardiovascular network. Time series were recorded in young and old healthy subjects, as well as post-acute myocardial infarction (AMI) patients, under orthostatic stress, which represents an exemplary testbed for the development and validation of analytical methods, due to the presence of well-defined oscillatory dynamics, measurable coupling mechanisms, and clinical relevance underlying autonomic and mechanical regulation. We hypothesized that the proposed metrics would be sensitive to changes in autonomic and mechanical cardiovascular mechanisms elicited by physiological maneuvers, as well as to regulation alterations related to aging and pathological states.

2. Methods

The proposed methodological framework was designed to quantify the dynamic coupling between two random processes and decompose it to assess entropy rate of each individual process as well as the directed information transfer between them. The framework included three main stages: (i) the estimation of MIR as a measure of dynamic stochastic interaction, and its decomposition into entropy rate and causality components, based on a data-efficient k-nearest neighbor estimator; (ii) the use of surrogate data analysis to assess the statistical significance of the estimated measures; (iii) the use of surrogate data analysis to evaluate the presence of nonlinearity in the evaluated dynamics.

The pipeline of analysis is schematized in Fig. 1, which provides a summary of the steps and their connections.

2.1. Mutual information rate

Let us consider a bivariate system $\mathcal{S} = \{\mathcal{X}, \mathcal{Y}\}$ composed of two interacting stationary and ergodic stochastic processes X and Y. For each process, it is possible to represent the current state as X_n and Y_n, where n is the time counter, and their past as $X_n^- = [X_{n-1}, X_{n-2}, \dots]$ and $Y_n^- = [Y_{n-1}, Y_{n-2}, \dots]$. This simple separation between present and past states allows us to explicitly consider the flow of time and to study causal interactions within and between processes by examining the statistical dependencies among these variables [42]. Furthermore, under the Markov assumption formulated with memory p, the past history of each process can be approximated with the p-dimensional vectors, i.e., $X_n^- \approx X_n^p = [X_{n-1}, X_{n-2}, \dots, X_{n-p}]$ and $Y_n^- \approx Y_n^p = [Y_{n-1}, Y_{n-2}, \dots, Y_{n-p}]$.

The MIR of the bivariate process composed of X and Y is defined as the limit, if it exists, of the rate at which the two dynamical systems exchange information per unit of time [35]:

$$I_{X;Y} = \lim_{p\to\infty} \frac{1}{p} I\left(X_n^p; Y_n^p\right), \tag{1}$$

where $I(\cdot;\cdot)$ is the mutual information.
Exploiting its formulation depending on entropy rates and the equivalence between entropy rates and conditional entropy valid for stationary processes, MIR can be decomposed in terms of: i) the complex behavior of the individual and joint systems; ii) the causal interactions between the two systems [43].

The first decomposition is given in terms of entropy rate quantities, which are expressed as the conditional entropy of the present state of a process given its own past history [39], i.e.,

$$\begin{aligned} I_{X;Y} &= H_X + H_Y - H_{X,Y} = \\ &= H(X_n|X_n^p) + H(Y_n|Y_n^p) - H(X_n, Y_n|X_n^p, Y_n^p), \end{aligned} \tag{2}$$

where $H(\cdot|\cdot)$ indicates the conditional entropy, H_X and H_Y are the entropy rates of the individual processes, and $H_{X,Y}$ their joint entropy rate.

The second decomposition is given in terms of measures of transferred information, which are indicative of causality related to past lags in both directions and to instantaneous causality. These quantities can be expressed through the conditional mutual information $I(\cdot;\cdot|\cdot)$, according to the following relation [39]:

$$\begin{aligned} I_{X;Y} &= T_{X\to Y} + T_{Y\to X} + I_{X\cdot Y} = \\ &= I(Y_n; X_n^p|Y_n^p) + I(X_n; Y_n^p|X_n^p) + I(X_n; Y_n|X_n^p, Y_n^p), \end{aligned} \tag{3}$$

where the transfer entropies $T_{X\to Y}$ and $T_{Y\to X}$ quantify the directed flow of information from process X to Y and from Y to X, respectively, and are closely related to the concept of Granger causality [30,44]. Transfer entropy indices allow to split the information flow in the two directions and to evaluate its asymmetry directly from the data, without a-priory assumptions on causal directions. The term $I_{X\cdot Y}$ represents the instantaneous (zero-lag) dependence between the two processes and constitutes a symmetric measure of instantaneous causality [43]. For the instantaneous term, it is important to clarify how a causal interpretation can be associated with it. Bearing in mind the principle that the cause must precede the effect, if prior knowledge about the analyzed dynamic system allows one to ascribe the instantaneous effect to one of the two directions of interaction, the instantaneous term of the decomposition (3) can be added to the corresponding transfer entropy, and the two

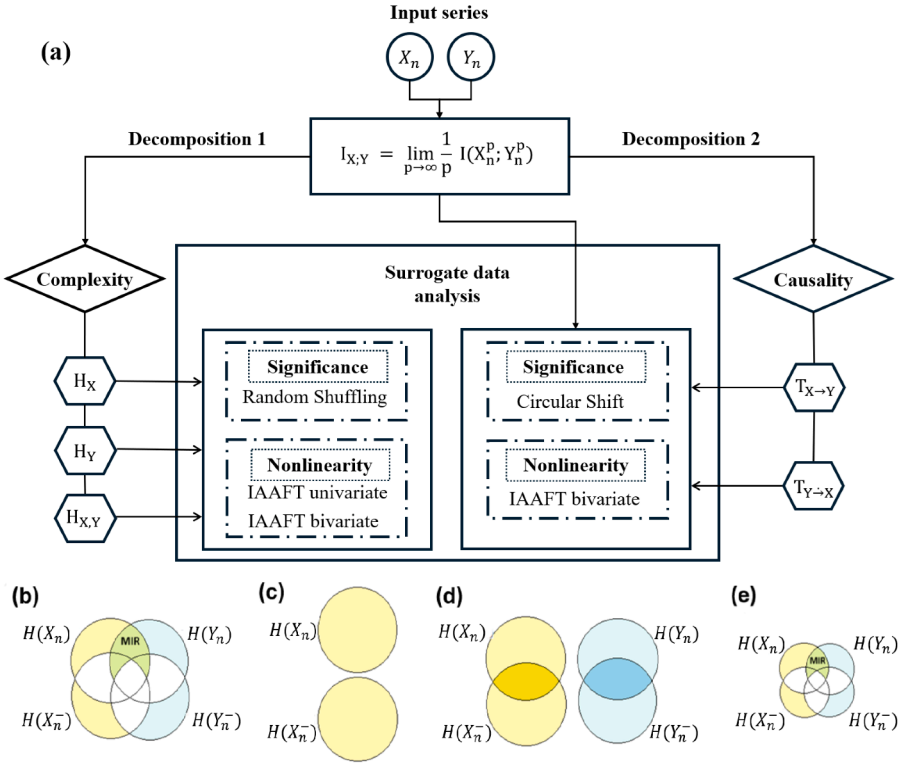

Fig. 1. Schematic representation of the proposed framework of analysis. (a) Estimation, decomposition, and assessment of the Mutual Information Rate (MIR). The input series X_n and Y_n are processed to estimate MIR, which is then decomposed into measures of complexity ($H_X + H_Y - H_{X,Y}$) and causality ($T_{X\to Y} + T_{Y\to X}$). (b-e) Venn diagrams illustrating surrogate-data analysis procedures. Specifically, (b) Shows the original coupling between two generic processes X (yellow) and Y (blue) as measured by MIR (green). (c) Random shuffling surrogates to test the statistical significance of complexity measures (example shown for X; analogous for Y). (d) Circular shift surrogates to test the statistical significance of MIR and causality measures. (e) IAAFT surrogates to detect nonlinear dynamics. Modified from [34].

can be treated as a single measure. Specifically, if prior physiological considerations allow to ascribe the instantaneous effects to the direction $Y \to X$, an aggregate measure of causal information transfer can be defined as: $T_{Y\dashrightarrow X} = T_{Y\to X} + I_{X\cdot Y}$. The two formulations provided in (2) and (3) facilitate the estimation of the MIR as a combination of conditional entropy and conditional mutual information terms.

All the information-theoretic quantities are expressed in nats, corresponding to the use of natural logarithms (base e) in entropy estimation.

2.2. Estimation of information measures

The nonparametric KNN estimator was adopted to compute the MIR and the complexity and causality terms into which MIR can be decomposed. The KNN estimator determines probability densities by evaluating the distances between each data point, representing a realization of the dynamic processes and its k-nearest neighbors in the observed space. According to the formalism introduced by *Kozachenko* and *Leonenko* [45], the entropy of a generic d-dimensional random variable V can be estimated as:

$$H(V) = -E[\ln p(\upsilon_n)] = \psi(N) - \psi(k) + d\langle \ln \epsilon_n \rangle, \tag{4}$$

where $E[\cdot]$ denotes the expectation operator, $\psi(\cdot)$ the digamma function, ϵ_n twice the distance between υ_n and its kth nearest neighbor determined using the maximum norm, and $\langle\cdot\rangle$ represents the average over all N observations of V.

Since MIR is computed by combining entropy terms defined over spaces of different dimension, the application of the same nearest neighbor search procedure in all spaces would produce heterogeneous search radii, when estimating probability densities, and an increasing bias, when terms are summed or subtracted. To mitigate this effect, the search distance can be kept constant in the higher-dimensional space, and projected onto the lower-dimensional spaces where the neighbors were counted, as proposed by *Kraskov, Stögbauer*, and *Grassberger* [46].

Accordingly, given two generic variables V and W and the possibility to decompose their conditional entropy and conditional mutual information in entropy $H(\cdot)$ and joint entropy $H(\cdot,\cdot)$ measures, i.e., $H(V|W) = H(V,W) - H(W)$ and $I(V;W|U) = H(V|U) - H(V|W,U)$, the terms in Eqs. (2) and (3) are estimated as [34,47]:

$$\begin{aligned} I_{X;Y} =& \psi(k) + \langle \psi(N_{X_n^p} + 1)\rangle + \langle \psi(N_{Y_n^p} + 1)\rangle - \langle \psi(N_{X_n X_n^p} + 1)\rangle \\ & - \langle \psi(N_{Y_n Y_n^p} + 1)\rangle - \langle \psi(N_{X_n^p Y_n^p} + 1)\rangle, \end{aligned} \tag{5}$$

$$H_X = \langle \psi(N_{X_n^p} + 1)\rangle - \langle \psi(N_{X_n X_n^p} + 1)\rangle + \langle \ln \epsilon_n \rangle, \tag{6}$$

$$H_Y = \langle \psi(N_{Y_n^p} + 1)\rangle - \langle \psi(N_{Y_n Y_n^p} + 1)\rangle + \langle \ln \epsilon_n \rangle, \tag{7}$$

$$H_{X,Y} = -\psi(k) + \langle \psi(N_{X_n^p Y_n^p} + 1)\rangle + 2\langle \ln \epsilon_n \rangle, \tag{8}$$

$$\begin{aligned} T_{X\to Y} =& \langle \psi(N_{Y_n^p} + 1)\rangle - \langle \psi(N_{Y_n Y_n^p} + 1)\rangle \\ & - \langle \psi(N_{X_n^p Y_n^p} + 1)\rangle + \langle \psi(N_{Y_n X_n^p Y_n^p} + 1)\rangle, \end{aligned} \tag{9}$$

$$\begin{aligned} T_{Y\dashrightarrow X} =& \psi(k) + \langle \psi(N_{X_n^p} + 1)\rangle - \langle \psi(N_{X_n X_n^p} + 1)\rangle \\ & - \langle \psi(N_{Y_n X_n^p Y_n^p} + 1)\rangle, \end{aligned} \tag{10}$$

where $\langle\cdot\rangle$ represents the average of N observations, $\psi(\cdot)$ is the digamma function, k the number of neighbors, ϵ_n twice the distance of each point from its kth neighbor in the space $[X_n, Y_n, X_n^p, Y_n^p]$, and N_Z is the number of neighbors whose distance from samples in the generic subspace Z is lower than $\epsilon_n/2$.

2.3. Surrogate data analysis

A multiple surrogate data approach was applied to assess the statistical significance and the nonlinearity of MIR and its decomposition metrics. Surrogate analysis is a hypothesis testing technique that compares measures computed on the original data with those obtained from surrogate series, which are generated to preserve all the characteristics of the original data except for the property under investigation, whose removal defines the null hypothesis [48]. In this study, four distinct types of surrogate series were generated to evaluate specific properties of the time series, as schematized in the Venn diagrams of Fig. 1. Specifically, two of these surrogate types were designed to assess statistical significance, i.e., Random shuffling and Circular shift, while the remaining two were intended to investigate the presence of nonlinear dynamics in both univariate and bivariate processes and are based on the Iterative Amplitude Adjusted Fourier Transform (IAAFT) procedure.

In detail, the statistical significance of the complexity measures (i.e., H_X, H_Y, and $H_{X,Y}$) was tested against the null hypothesis that the time series were realizations of a process that did not exhibit self-dependencies (i.e., $H_X = H(X_n)$). To this aim, *Random Shuffling* surrogate series were generated by independently and randomly permuting the samples of each time series, thereby destroying any temporal structure of the original series while preserving their marginal distributions (Fig. 1(c)). The statistical significance of the causality measures (i.e., $T_{X\to Y}$, $T_{Y\to X}$) and of the MIR was tested against the null hypothesis that the two time series originated from statistically independent processes (i.e., $I_{X;Y} = 0$). In this case, *Circular Shift* surrogate data were generated, which destroyed the coupling between the two series introducing a random temporal shift, bigger than the Markov memory of one of the two series, but preserved the statistical properties of each individual series, as illustrated in Fig. 1(d).

The presence of nonlinearity in univariate metrics (i.e., H_X, H_Y) was tested against the null hypothesis that the series originated from Gaussian linear stochastic processes. The *IAAFT* surrogates were generated, which preserved both the empirical amplitude distribution and the power spectrum of the signal series (i.e., their linear properties), while destroying nonlinear temporal dependencies [49]. The same approach was extended to the bivariate measures (i.e., $H_{X,Y}$, $T_{X\to Y}$, $T_{Y\to X}$, MIR) to test the presence of nonlinearity against the null hypothesis that the observed interdependence was solely due to linear interactions. Bivariate IAAFT surrogates were generated by applying the same random phase shift to the Fourier components of both series, thus preserving not only individual spectra but also their cross-spectral structure, while disrupting the nonlinear correlation between the past and present states. Fig. 1(e) graphically represents this surrogate procedure using a Venn diagram, where the smaller intersection between the two processes indicates that the dependence between the past and present is not completely destroyed, but it is different from the original case in Fig. 1(b) because only linear correlations are retained [48].

To assess the reliability of the metrics, for each pair of time series, a surrogate distribution was generated by repeating M times the specific surrogate generation procedure. The information-theoretic measure of interest was computed on both the original series and each surrogate series. A non-parametric percentile-based test was adopted to assess statistical significance based on 5% significance level. Conditional entropy measures were deemed significant if the value computed on the original series fell below the 5th percentile of the surrogate distribution derived from *Random Shuffling*. Mutual information measures were considered significant if the original value exceeded the 95th percentile of the distribution obtained from *Circular Shift* surrogates [41,48]. For *IAAFT* the null hypothesis was rejected if the original value fell below the 5th percentile for univariate processes, or exceeded the 95th percentile of the surrogate distribution for bivariate processes, thereby indicating the presence of nonlinear dynamics either within or between the processes [34,49,50].

3. Application to physiological time series

The analytical framework described above was applied to the previously collected GISSI-3 study database of cardiovascular time series [51–53], to assess its capability to highlight changes in entropy rate, causality, and nonlinearities of the cardiovascular dynamics across different physiological and pathophysiological conditions. Specifically, RR and SAP recordings from young healthy subjects, older healthy individuals, and post-AMI patients were analyzed during a tilt-induced orthostatic stress, to assess how information dynamics adapt with aging and in the presence of cardiac pathology.

3.1. Data acquisition and time series extraction

The GISSI-3 study was conducted in accordance with the Declaration of Helsinki and each subject provided written informed consent. The database included cardiovascular signals, acquired from 35 post-AMI patients (58.5 ± 10.2 years, 4 females), examined 10 ± 3 days after the event, and from two groups of healthy subjects composed of 19 young (25.0 ± 2.6 years, 9 females) and 12 old (63.1 ± 8.3 years, 9 females) subjects. Post-AMI patients were part of the larger database collected for a GISSI-3 arrhythmia substudy [51,54]. Eight patients were treated with β-blockers, which were discontinued two half-lives before the recordings. All healthy subjects were normotensive and free of known diseases. Recordings were performed after 15 min in a resting baseline condition and included electrocardiographic (ECG, Siemens Mingograph, lead II, bandwidth 0.3–1000 Hz) and arterial blood pressure (ABP) signals, the latter measured at the finger using a Finapres photoplethysmograph (Ohmeda 2300). Each acquisition consisted of 10 min in the supine position (REST) and 10 min during passive head-up tilt at 60° (TILT). Signals were digitized at 12-bit resolution and 1 kHz sampling frequency.

From the recorded signals, physiological time series indicative of cardiovascular dynamics were extracted. Specifically, RR intervals were extracted by detecting R peaks in the ECG via template matching and considering the temporal distances in between, while SAP was computed as the maximum pressure value within each detected cardiac cycle. For each subject and experimental condition, the series were cleaned from artifacts, windowed to 300 samples (~5 min) and detrended using a zero-phase autoregressive high-pass filter to remove slow trends. Stationarity was assessed by visual inspection. Finally, RR and SAP time series were standardized by z-score normalization. The mean and standard deviation of the time series before standardization are reported in Table 1S of the Supplementary Material.

Further details on the experimental protocol and data acquisition are provided in [32,51].

3.2. Data and statistical analysis

The MIR framework was applied to cardiovascular time series, treating RR intervals and SAP as processes X and Y, respectively. Global coupling, entropy rate of cardiac and vascular dynamics, and causal interactions between RR and SAP were assessed. The instantaneous term was associated with the causal direction $SAP \to RR$, since, by construction of the time series the peak of systolic arterial pressure (SAP_n) occurs before the end of the RR_n interval (see Fig. 2(a)). This temporal arrangement of the time series suggests that SAP_n may influence the duration of RR_n within the same cardiac cycle, thus incorporating the instantaneous term of the interaction related to the fast baroreflex modulations.

The joint evaluation of the instantaneous effect and of the causal measure accounting only for the past history of the source follows the approach adopted in previous studies, which demonstrated that their combination provides a more realistic description of the dynamics underlying baroreflex responses [10]. All metrics were estimated using the KNN approach with $k = 10$ and $p = 3$ samples for past history reconstruction. These parameter values were selected in accordance with previous

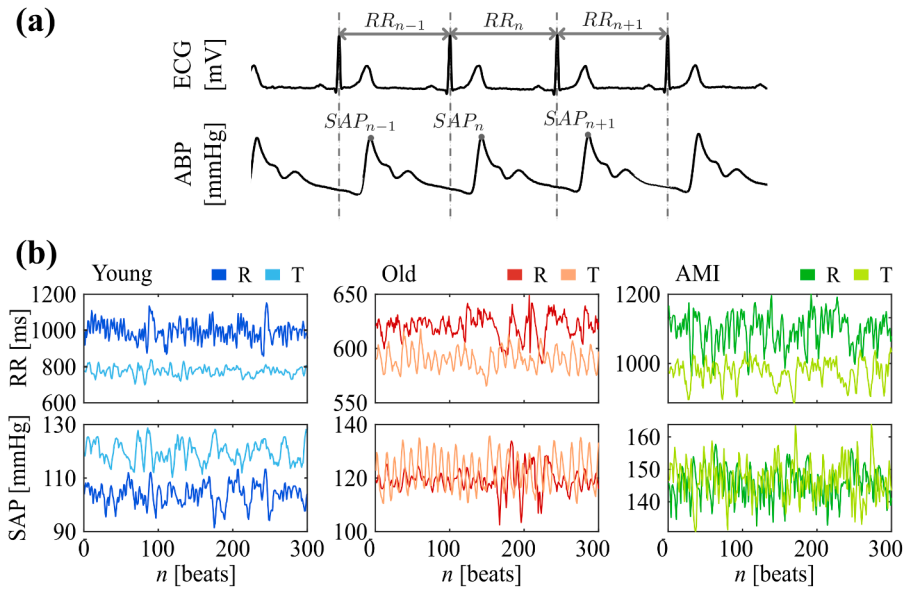

Fig. 2. (a) Representative segments of the electrocardiographic (ECG) and arterial blood pressure (ABP) signals illustrating the extraction of RR and systolic arterial pressure (SAP) time series. (b) Example of RR and SAP series from a representative subject of each group during REST (R) and TILT (T). Please, note that the y-axis range is different in different subjects.

studies on cardiovascular dynamics [33,55]. In particular, the choice of the lags allowed to consider physiological mechanisms acting very fast, as well as effects distributed over subsequent cycles. To evaluate the effects of the parameter choice and to assess the stability of the results, a sensitivity analysis was conducted by varying one parameter at a time. First, MIR, entropy rate, and causality indices were calculated fixing the embedding dimension at $p = 3$ and varying the number of neighbors within the set $k = 5$, 10, and 20. Then, k was fixed at 10 and the embedding dimension changed within the set $p = 2$, 3, and 4.

Surrogate data analysis was performed generating $M = 100$ surrogate series for each subject and condition to test the statistical significance and nonlinearity of the measures. For each experimental group and condition, the results of surrogate analysis were expressed in terms of the percentage of subjects for whom the corresponding null hypothesis was rejected ($p < 0.05$).

For each group, the comparison between rest and orthostatic stress states was evaluated using the Wilcoxon signed-rank test [56]. Moreover, to assess whether the proportion of significant or nonlinear results differed across conditions, a chi-squared test on 2×2 contingency tables was applied [51]. Finally, between-group comparisons were performed separately for REST and TILT. Specifically, the Kruskal-Wallis test [57] was used to assess differences among the three groups. When significant, pairwise comparisons were carried out with the Wilcoxon rank-sum test adjusted by Bonferroni correction for multiple comparisons ($n = 3$) [58,59], evaluating statistically significant variations between Young vs. Old, Old vs. AMI, and Young vs. AMI. A p-value lower than 0.05 was considered statistically significant for all the statistical analysis.

4. Results

4.1. Global coupling: MIR

The characterization of cardiovascular dynamics in terms of global coupling, as provided by MIR values, is shown in Fig. 3. Panel (a) shows the comparison of MIR values between the REST and TILT conditions for the three groups of young subjects, old subjects, and post-AMI patients, while panel (b) shows the percentage of subjects exhibiting nonlinear dynamics (i.e., those for whom the null hypothesis of purely linear dynamics was rejected), assessed through *IAAFT_bivariate* surrogates.

Global cardiovascular coupling values (panel (a)) did not exhibit significant variations with postural stress in young subjects and AMI patients, while a statistically significant increase in MIR was observed in old subjects. MIR was significantly lower in old and post-AMI patients compared to young subjects at REST. The difference persisted under stress conditions in post-AMI patients. The assessment of MIR through the *Circular Shift* surrogate analysis confirmed the statistical significance in around 100% of subjects across all groups and in both experimental conditions (data not shown).

The assessment of nonlinearity by *IAFFT* surrogate analysis in panel (b) pointed out a significant decrease in the percentage of patients exhibiting nonlinear dynamics in global cardiovascular coupling during TILT in young subjects, while minor changes were observed in old subjects and AMI patients.

4.2. Decomposition 1: entropy rates

Fig. 4 illustrates the results of the decomposition of MIR into entropy rate measures of cardiac (a), vascular (c), and cardiovascular (e) dynamics assessed in terms of entropy rate. For each measure, comparisons are shown between the two experimental conditions in the different subject groups. For each metric, the percentages of subjects exhibiting nonlinear dynamics, as assessed through *IAAFT_univariate* surrogates (b, d) or *IAAFT_bivariate* surrogates (f), are displayed in the corresponding right panels.

Panel (a) shows that cardiac entropy rate (H_{RR}) decreased in all groups following orthostatic stress, although the variation reached statistical significance only in young subjects. The intergroup comparison revealed significantly higher H_{RR} values in old subjects and AMI patients compared to young subjects under orthostatic stress.

In panel (c), the vascular entropy rate (H_{SAP}) showed a statistically significant decrease in young subjects with TILT, whereas a non significant increase were observed in old subjects and post-AMI patients. The intergroup comparison showed significantly higher H_{SAP} values in old and post-AMI patients compared to young subjects during TILT, and in post-AMI patients compared to old subjects at REST.

In panel (e), the joint conditional entropy $H_{RR,SAP}$ showed a statistically significant decrease in young subjects during TILT, while only minor changes occurred in old subjects and post-AMI patients. The

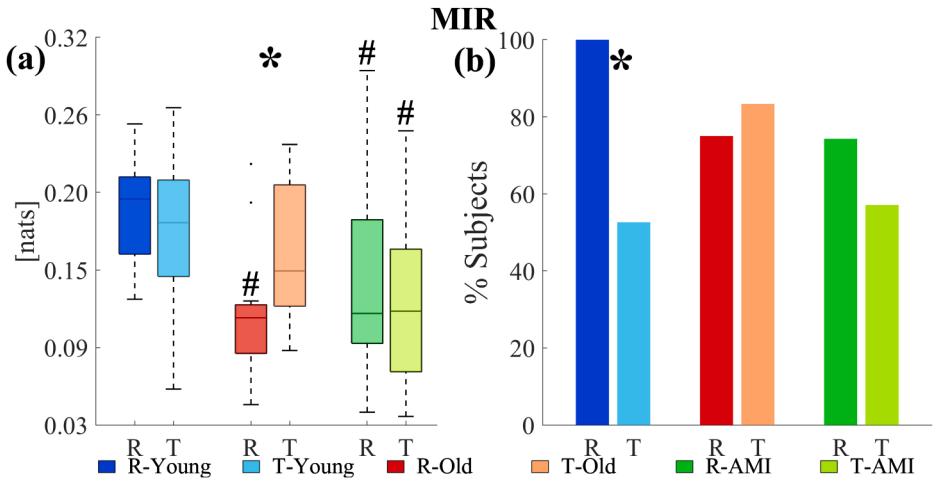

Fig. 3. Analysis of the global cardiovascular coupling assessed by MIR, $I_{RR;SAP}$, at REST (R) and during TILT (T) in the three study groups: (a) boxplots of MIR in the two experimental conditions in young (blue), old (red) and post-AMI (green) populations; (b) percentage of subjects exhibiting nonlinear dynamics, as assessed by IAFFT surrogates. Statistical test REST vs. TILT: *, $p < .05$, paired Wilcoxon signed-rank test; between group comparison vs. Young #, $p < .05/3$, post-hoc Wilcoxon rank-sum test adjusted by Bonferroni correction; *, $p < .05$, chi-squared test.

intergroup comparison revealed a significantly higher $H_{RR,SAP}$ in old and post-AMI patients compared to young subjects during TILT.

The assessment based *Random Shuffling* surrogates confirmed significance for all the metrics in around 100% of subjects, under both experimental conditions (data not shown).

Regarding nonlinearity, a reduction in the percentage of patients with nonlinear dynamics was observed in old subjects during TILT, which reached statistical significance for cardiac entropy rate (b). No relevant changes were observed in the other two groups.

4.3. Decomposition 2: causality

Fig. 5 shows the results of the second decomposition of MIR into causality measures. Panels (a,c) report the values of $T_{RR\to SAP}$ and $T_{SAP\dashrightarrow RR}$ in the two experimental conditions for the three groups. Panels (b,d) display the percentage of subjects exhibiting nonlinear dynamics, as assessed through *IAAFT_bivariate* surrogates.

In panel (a), $T_{RR\to SAP}$ was significantly reduced in young subjects during TILT. Intergroup comparison showed significantly lower values in old subjects compared to young subjects at REST.

In panel (c), $T_{SAP\dashrightarrow RR}$ values showed a statistically significant increase in old subjects with TILT. In addition, although not shown in the figure, when excluding the instantaneous causality term, a significant increase was also observed in young subjects. In the intergroup comparison, old and post-AMI patients exhibited significantly lower values than young subjects at REST, whereas, during TILT, post-AMI patients displayed significantly lower values than both young and old subjects.

The assessment of information transfer significance by *Circular Shift* surrogates showed a small percentage of patients with significant $T_{SAP\dashrightarrow RR}$ values in old subjects, which significantly increased during TILT (REST $\simeq$ 33%, TILT $\simeq$ 92%). Although not statistically significant, an increase was observed in young subjects (REST $\simeq$ 84%, TILT $\simeq$ 95%), and an opposite trend was found in post-AMI patients (REST $\simeq$ 62%, TILT $\simeq$ 57%), which was also not statistically significant. For the $T_{RR\to SAP}$ measure, all subjects showed a significance value of more than 90% in both conditions (data not shown).

Regarding nonlinearity (panels (b) and (d)), a statistically significant reduction of the percentage of subjects displaying nonlinear dynamics in information transfer was observed during TILT in young group along both RR to SAP and SAP to RR directions, whereas a significant increase in nonlinear dynamics was observed in old subjects along the SAP to RR direction.

4.4. Results of sensitivity analysis

The results of sensitivity analysis are summarized in Figures 1S and 2S in the Supplementary Material. Figure 1S shows the behaviour of the indices when changing the number of neighbours k. The increase of k led to a reduced variability and a slight decrease in the magnitude of the estimated measures. Overall, the main patterns remained qualitatively stable across different configurations, with only minor statistical differences depending on the choice of k. Figure 2S shows the behaviour of the indices when changing the embedding dimension p. The increase of p resulted in a moderate reduction in the absolute values of MIR and causality measures, likely due to increased sparsity in the reconstructed space. The main reduction occurred between $p = 2$ and $p = 3$, while effects were minor between $p = 3$ and $p = 4$, with only minor alterations in the overall patterns.

5. Discussion

This work presented the implementation and application of an analytical framework, combining the advantages of a KNN-based estimation of MIR and its decomposition with the analysis of four different types of surrogates, on heart period and systolic arterial pressure data. The combination granted a reliable quantification of entropy rate, causality, and nonlinearity in cardiovascular dynamics assessed across different pathophysiological states.

5.1. Framework to assess dynamic coupling, entropy rate, and causality in short bivariate time series

MIR is a statistical and information theoretic measure of dependence and directional information flow between two time series, which are observable manifestations of the underlying physiological mechanisms. Measures like MIR [32,33] are important because they allow to quantify the coupling between dynamic processes in a model-free fashion. Despite being theoretically well established, the MIR has received limited attention by practitioners, primarily due to the difficulty of estimating it reliably from short time series and of assessing its significance level. Moreover, its relation with measures of complexity of the coupled dynamics, or with measures of causal information flow, was not typically exploited.

The framework proposed in this work formalizes the link between measures of dynamic coupling, entropy rate, and causality within the MIR decomposition. Specifically, the MIR can be expressed as the sum

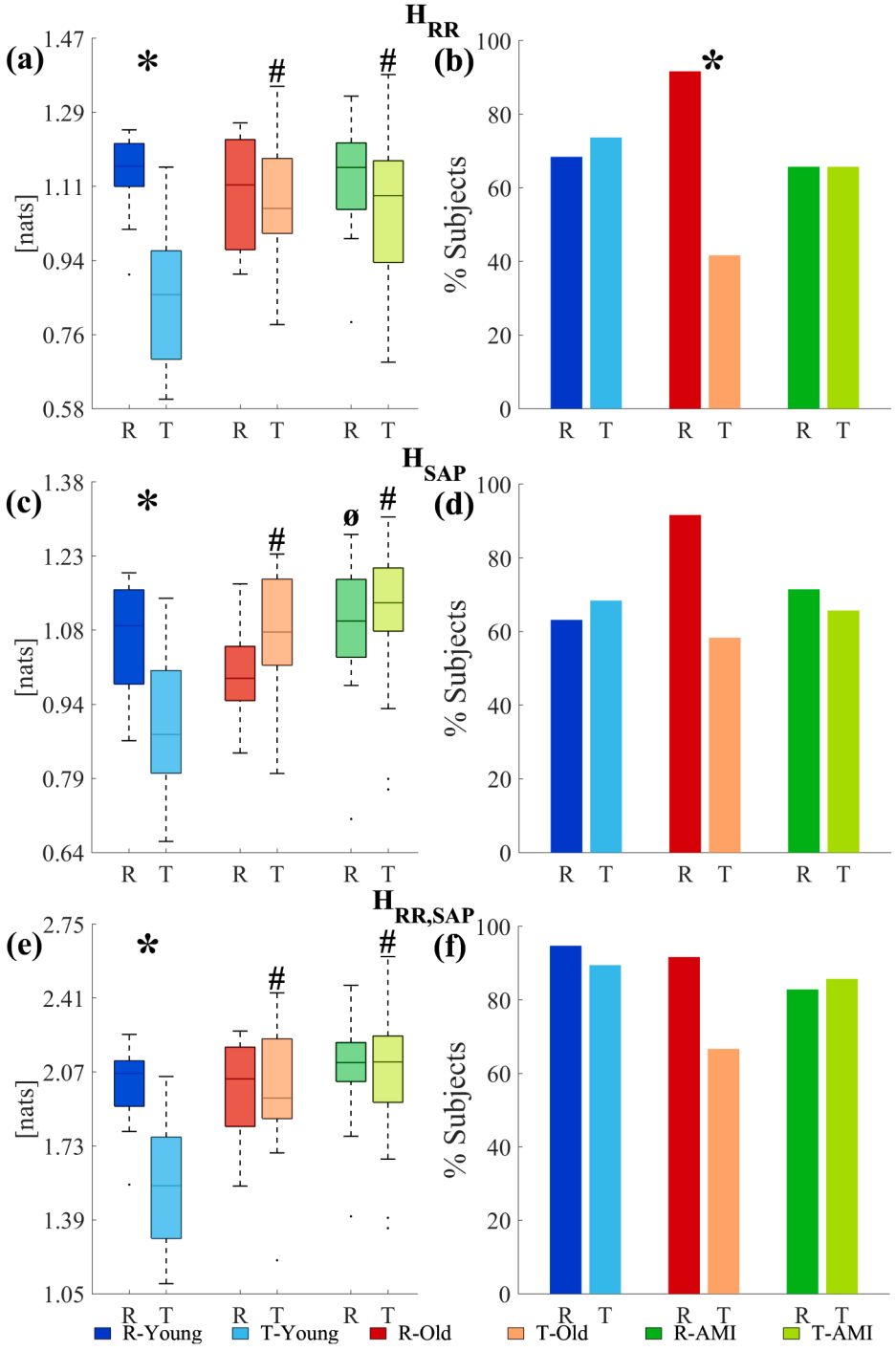

Fig. 4. MIR decomposition into entropy measures at REST (R) and during TILT (T) in the three study groups: (a, c, e) boxplots of cardiac (H_{RR}), vascular (H_{SAP}), and cardiovascular entropy rate ($H_{RR,SAP}$) measures in the two experimental conditions in young (blue), old (red) and post-AMI (green) populations; (b, d, f) percentage of subjects exhibiting nonlinear dynamics, as assessed by IAFFT surrogates. Statistical tests: REST vs. TILT: *, $p < .05$, paired Wilcoxon signed-rank test; between group comparison vs. Young #, and vs. Old Ø, $p < .05/3$, post-hoc Wilcoxon rank-sum test adjusted by Bonferroni correction; *, $p < .05$, chi-squared test.

of the individual entropies minus the joint entropy of the observed processes, or as the sum of the bidirectional transfer entropy measures and the instantaneous information at zero lag. This formulation enables a unified quantification of the information shared between interacting processes, distinguishing between delayed causal interactions and instantaneous (possibly common-driver or feedback-related) effects. To enhance interpretability, when physiological knowledge supports a directional information flow, the instantaneous interaction term was incorporated into one of the two transfer entropy measures, providing a more coherent representation of causal dependencies.

In this work, MIR-based metrics were estimated using the KNN estimator, which offers several advantages. First, it avoids the strong distributional assumptions inherent in parametric linear models and enables the detection of nonlinear dependencies that Gaussian models typically fail to capture [55,58,60]. Second, it reduces the discretization bias introduced by binning or permutation based approaches [33,56,57].

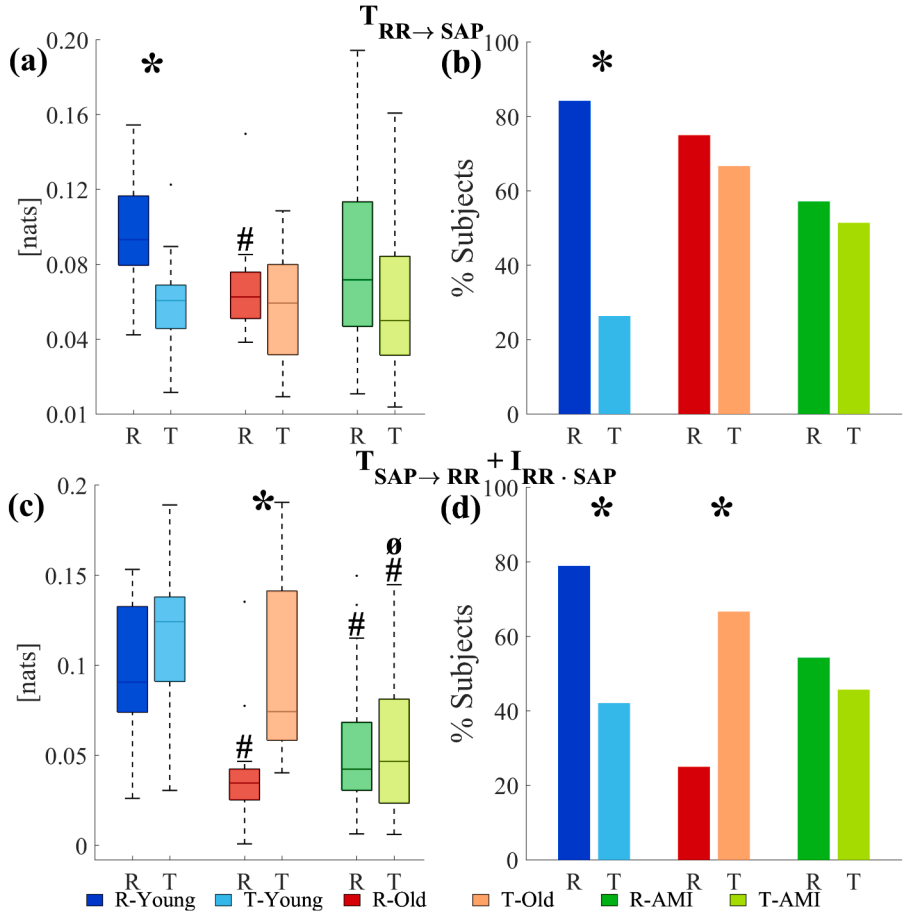

Fig. 5. MIR decomposition into causality measures at REST (R) and during TILT (T) in the three study groups: (a, c) boxplots of causality measures ($T_{RR\to SAP}$, $T_{SAP\to RR}$) for the two experimental conditions in young (blue), old (red) and post-AMI (green) populations; (b, d) percentage of subjects exhibiting nonlinear dynamics, as assessed by IAAFT surrogates. Statistical tests REST vs. TILT: *, $p < .05$, paired Wilcoxon signed-rank test; between group comparison vs. Young #, and vs. Old Ø, $p < .05/3$, post-hoc Wilcoxon rank-sum test adjusted by Bonferroni correction; *, $p < .05$, chi-squared test.

However, the estimator is sensitive to the choice of the embedding dimension p and the number of neighbors k. For this reason, the parameter values ($p = 3$, $k = 10$) were selected based on previous studies on cardiovascular dynamics [29,61], and the stability of the results was assessed by sensitivity analysis. In particular, the interplay between sample size, embedding dimensionality, and neighborhood size affects the bias-variance balance of KNN estimators, as pointed out also by the results of the sensitivity analysis. The choice of k involves a trade-off between variance and bias, where increasing k reduces the variance but increases the bias. The choice of a low embedding dimension ($p = 3$) was operated to mitigate the bias on the estimates associated with the curse of dimensionality [34,62], while preserving sensitivity to the underlying dynamics. Overall, the selected configuration represents a compromise between estimation stability and dimensionality of the reconstructed space [33,55]. However, the optimization of embedding parameters in short time series remains an open issue, and computational costs increase with dimensionality, potentially limiting real-time applicability [61].

The integration of the MIR framework with four different surrogate data types was crucial to ensure robust statistical validation of significance and nonlinearity of the computed complexity and causality metrics. In this context, a key advantage of the MIR decomposition lies in the possibility of validating each component through surrogate testing, thereby obtaining statistically significant estimates and physiologically consistent interpretations even under nonlinear dynamics. Among the surrogate strategies, the IAAFT proved particularly effective in identifying nonlinear components in the observed dynamics. It is worth noting that the nonlinearity assessment provided in this study should not be regarded as a measure of a residual nonlinear component of the indices, but instead interpreted in terms of a violation of the linear null hypothesis assessed through IAAFT surrogate analysis, which preserves the linear properties of RR and SAP while removing higher-order dependencies [41]. In this sense, the IAAFT-based analysis does not allow a separation between linear and nonlinear dynamics, but rather enables the evaluation of whether nonlinear dynamics play a relevant role in determining RR-SAP coupling under the investigated conditions. When such nonlinear contributions are observed in a significant proportion of subjects, they may question the adequacy of classical linear analyses (e.g., correlation or coherence), which should therefore be complemented, or potentially replaced, by nonlinear or model-free approaches such as the one adopted in this study.

5.2. *Characterization of nonlinear cardiovascular dynamics across pathophysiological states*

The proposed analysis framework was tested on cardiovascular series to evaluate its capability to track cardiac and vascular dynamics in response to orthostatic stress across different subject groups. Our results confirmed changes well-documented in the literature, but disclosed also subtle nonlinear aspects that are less explored.

In young healthy subjects, the analysis of global coupling suggested the preservation of a functional balance between the cardiac and vascular systems in response to orthostatic stress, while MIR-decomposition measures disclosed branch modulation. The entropy rate reduction

observed with TILT is consistent and extends with previous studies [5,27,32,63–65], which provided evidence that the TILT maneuver induced a shift of the sympatho-vagal balance towards a sympathetic activation with a reduction in the harmonic modulation of heart rate and a reduction of the baroreceptor loading. Similarly, causality measures were consistent with the literature, which highlighted an increase in the flow of information from SAP to RR and a decrease in the opposite direction [33,51]. This pattern is consistent with the presence of a closed-loop interaction in cardiovascular regulation and the reweighting of its two branches during the TILT maneuver [28,66,67]. In particular, the strengthening of information transfer from SAP to RR (partially obscured by adding the instantaneous causality term may reflect the action of the baroreflex regulation mechanism, whereas the opposite direction may be associated with the feedforward components [27,51].

In old subjects, lower MIR and causality values than in young individuals were observed at REST. This pattern suggests reduced flexibility of the autonomic system and a potential impairment of cardiovascular compensatory mechanisms, which is consistent with the physiological framework of "loss of complexity" in aging reported in the literature [68–70]. The interpretation of the respose during TILT requires a closer look. In terms of transfer entropies, old subjects did not present the decrease in $T_{RR\to SAP}$ observed in young subjects, since their levels were already low at rest. However, they still manifested a response to the manouvre with a significant increase of $T_{SAP\to RR}$. The partial preservation of a dynamic structure correlated to autonomic patterns in old subjects, albeit with blunted amplitude with respect to the young ones, has been previously observed in other physiological states, such as the alternation between sleep and wake states [7,70–72]. On the other hand, entropy values pointed out peculiar characteristics of the response to TILT in old subjects with respect to young ones. Young subjects exhibited a reduction in entropy rate measures during TILT, while older subjects showed higher entropy values than young subjects, particularly for H_{SAP}. The higher unpredictability of the series during TILT should not be interpreted in itself as either an improvement or a deterioration of cardiovascular regulation, but rather as an alteration and reorganization of cardiovascular dynamics under orthostatic stress. This trend is in line with previous studies [73,74],which indicate that old individuals having less flexible cardiovascular compensatory mechanisms, may necessitate to recruit multiple regulatory strategies, to maintain a certain degree of hemodynamic stability. Indeed, it is well known that with advancing age, systolic pressure becomes less stable due to reduced baroreflex sensitivity, a decrease in the number, density, and sensitivity of cardiac β-adrenergic receptors [20], as well as an increase in arterial stiffness.

In post-AMI patients at REST, a behavior similar to that of the old group was observed, attributable to the comparable age of the two populations. However, unlike the elderly, post-AMI patients showed no significant modulation of MIR, and its decomposition during orthostatic stress. These differences may be attributed to the acute cardiac event, which induces an inflammatory state and oxidative stress further impairing endothelial and autonomic function; ventricular remodeling and altered sympathetic innervation, together with pharmacological therapies, can contribute to autonomic imbalance [21,75,76].

A distinctive feature and selective advantage of our framework is the possibility to assess the contribution of nonlinear mechanisms to the observed dynamics. These are essential for a deeper understanding of control and adaptation mechanisms of the body in response to external stimuli, as nonlinear interactions between sympathetic and parasympathetic systems play a crucial role in cardiovascular regulation [22,35,55].

Specifically, the reduction of nonlinearity in young subjects with TILT, observed in both global coupling and causality measures, are well established results in the literature, converging on the evidence that these subjects exhibit a stronger sympathetic drive [32,77,78] and a more adaptive autonomic nervous system in response to external stimuli compared to the other groups.

In old subjects, the increase in nonlinear dynamics involved in the baroreflex mechanism and the decrease of cardiovascular dynamics reflect a less adaptive response to orthostatic stress. These findings are in line with [32], confirming that aging is associated with reduced efficiency of autonomic regulatory mechanisms.

Unlike young and old subjects, in post-AMI patients, no relevant modulation of nonlinear mechanisms was observed in response to orthostatic stress. The literature indicates that this behavior can be partly attributed to the effect of pharmacological therapy [79–81]. Moreover, lower percentages of patients with nonlinear dynamics (both at REST and during TILT) were found compared to young subjects. This result, consistent with previous results in terms of Information Storage applied to RR series [32], suggests that in pathological conditions heart rate variability dynamics tend to become more linear and predictable, reflecting a reduced ability of the organism to respond to external stimuli.

5.3. Limitations and future development

The proposed method is based on a bivariate characterization of time series interactions, and it does not allow to consider the potential influence of additional variables on the two series and their coupling, nor to distinguish between direct and indirect interactions. In the presented application, it yielded a focused investigation of RR-SAP coupling, which however represents only a partial projection and reduced representation of the underlying multivariate physiological network. Accordingly, physiological interpretation should be approached with caution, as results may depend on the adopted methodology and on the reduced multivariate representation. Cardiovascular variability arises from the interaction of multiple control mechanisms. Among these, respiration may plays a modulating role on heart rate variability and on baroreflex regulation, influencing the joint dynamics of heart rate and arterial pressure [4–7]. In this perspective, future studies may apply the same framework to other pairs of physiological signals, e.g., cardiac and respiratory series, in order to explore additional interactions between different regulatory mechanisms and provide a more complete picture of the interactions. The method could also be applied to other physiological models of autonomic modulation, such as transitions between sleep stages, where changes in the nonlinear components of cardiac dynamics have been widely reported [7,70–72]. Future studies should include comparison of MIR and entropy rate with other nonlinear metrics [70–72], as entropy rate mainly reflects short-term unpredictability and fails to capture multiscale physiological complexity driven by long-range correlations and nonlinear interactions. From a methodological perspective, future work should include a systematic comparison between the KNN-based estimator and alternative entropy and transfer entropy estimators (i.e., Kernel, Binning or Permutation estimators), in order to better characterise the trade-off between computational efficiency, robustness to noise, and sensitivity to nonlinear dynamics.

6. Conclusion

This study proposed the combined use of stochastic interaction decomposition strategies and multiple surrogate data analysis to provide a comprehensive characterization of cardiovascular system dynamics in terms of entropy rate, causality, and nonlinearity features. The evaluation of the framework on a testbed of RR interval and SAP time series, recorded under well-known physiological and pathophysiological conditions, supported the capability of the framework to capture meaningful changes in cardiovascular dynamics across healthy and altered functional states. In young healthy individuals, stress induced reduction in entropy rate, increased sympathetic activation, enhanced baroreflex causality, and a tendency toward linearization, which are consistent with an effective and flexible autonomic response. Extending the analysis to old subjects and AMI patients provided insight into the deterioration of cardiovascular regulation. Old individuals showed increased entropy but reduced coupling and nonlinear modulation, suggesting reduced baroreflex efficiency and increased arterial stiffness. In post-AMI patients, coupling and predictability were markedly reduced,

with minimal modulation under stress, pointing out an impaired autonomic control, potentially influenced by residual pharmacological effects and structural alterations. Our results demonstrate the potential of this framework to provide sensitive descriptors of cardiovascular regulation across different physiological and pathological conditions. Application to larger and more diverse populations is however necessary to understand the potential role of these metrics to support early diagnosis, risk stratification, and personalized treatment strategies in cardiovascular medicine.

CRediT authorship contribution statement

Stefano Cimignolo: Writing – original draft, Visualization, Software, Investigation, Formal analysis; **Chiara Barà:** Writing – review & editing, Visualization, Validation, Software; **Riccardo Pernice:** Writing – review & editing, Validation, Software; **Luca Faes:** Writing – review & editing, Validation, Software, Methodology, Conceptualization; **Giandomenico Nollo:** Writing – review & editing, Supervision, Resources, Data curation; **Michela Masè:** Writing – review & editing, Validation, Supervision, Methodology, Conceptualization.

Declaration of competing interest

The authors declare that they have no known competing financial interests or personal relationships that could have appeared to influence the work reported in this paper.

Acknowledgment

This work was supported by the project “HONEST- High-Order Dynamical Networks in Computational Neuroscience and Physiology: an Information-Theoretic Framework”, Italian Ministry of University and Research (funded by MUR, PRIN 2022, code 2022YMHNPY, CUP: B53D23003020006), and by the MUR PNRR project INEST- Interconnected Nord-Est Innovation Ecosystem (ECS00000043) funded by the NextGenerationEU.

Supplementary material

Supplementary material associated with this article can be found, in the online version, at 10.1016/j.bbe.2026.07.003

References

[1] World Health Organization. Cardiovascular diseases (CVDs). Accessed: 2025-10-15, https://www.who.int/news-room/fact-sheets/detail/cardiovascular-diseases-(cvds); .
[2] La Rovere MT, Pinna GD, Raczak G. Baroreflex sensitivity: measurement and clinical implications. Ann Noninvasive Electrocardiol: Off J Int Soc Holter Noninvasive Electrocardiol Inc 2008;13(2):191–207.
[3] Stanfield CL. Principles of human physiology. Pearson; 2011.
[4] Wessel N, Riedl M, Kurths J. Is the normal heart rate "chaotic" due to respiration? Chaos 2009;19:028508. https://doi.org/10.1063/1.3133128
[5] Halliwill J, Morgan B, Charkoudian N. Peripheral chemoreflex and baroreflex interactions in cardiovascular regulation in humans. J Physiol 2003;552:295–302. https://doi.org/10.1113/jphysiol.2003.050708
[6] Nardone M, Teixeira A, Incognito A, Vermeulen T, Shafer B, Millar P, et al. Within-breath sympathetic baroreflex sensitivity is modulated by lung volume but unaffected by acute intermittent hypercapnic hypoxia in men. Am J Physiol-Heart Circ Physiol 2020;319. https://doi.org/10.1152/ajpheart.00296.2020
[7] Schumann AY, Bartsch RP, Penzel T, Ivanov PC, Kantelhardt JW. Aging effects on cardiac and respiratory dynamics in healthy subjects across sleep stages. Sleep 2010;33(7):943–55. https://doi.org/10.1093/sleep/33.7.943
[8] Eckberg D. Topical review: the human respiratory gate. J Physiol 2003;548. https://doi.org/10.1111/j.1469-7793.2003.00339.x
[9] Katona PG, Jih F. Respiratory sinus arrhythmia: noninvasive measure of parasympathetic cardiac control. J Appl Physiol 1975;39(5):801–5. https://doi.org/10.1152/jappl.1975.39.5.801
[10] Faes L, Porta A, Nollo G. Information decomposition in bivariate systems: theory and application to cardiorespiratory dynamics. Entropy 2015;17(1):277–303.
[11] Ivanov PC. The new field of network physiology: building the human physiolome. Front Netw Physiol 2021;1.
[12] Saladin KS. Anatomia umana. Piccin; seconda edizione italiana sulla quinta americana ed.; 2017.
[13] Hennis K, Biel M, Wahl C, Fenske S. Beyond pacemaking: HCN channels in sinoatrial node function. Prog Biophys Mol Biol 2021;166:51–60.
[14] Sherwood L. Human physiology: from cells to systems. Cengage Learning; 7th ed.; 2010.
[15] Augustin CM, Gsell MAF, Karabelas E, Plank G. Physiologically valid 3D-0D closed loop model of the heart and circulation – modeling the acute response to altered loading and contractility. arXiv: Tissues and Organs, 2020. https://api.semanticscholar.org/CorpusID:221802454
[16] Shaffer F, Venner J. Heart rate variability anatomy and physiology. Biofeedback 2013;41:13–25.
[17] Javorka M, Czippelova B, Turianikova Z, Lazarova Z, Tonhajzerova I, Faes L. Causal analysis of short-term cardiovascular variability: state-dependent contribution of feedback and feedforward mechanisms. Med Biol Eng Comput 2017;55:179–90.
[18] Chaui-Berlinck JG, Monteiro L HA. Frank-starling mechanism and short-term adjustment of cardiac flow. J Exp Biol 2017;220(23):4391–8.
[19] Ardell JL, et al. Activity of in vivo atrial and ventricular neurons in chronically decentralized canine hearts. Am J Physiol 1991;260(3 Pt 2):H713–H721.
[20] Chaddha A, Rafanelli M, Brignole M, Sutton R, Wenzke KE, Wasmund SL, et al. The pathophysiologic mechanisms associated with hypotensive susceptibility. Clin Auton Res 2016;26(4):261–8.
[21] Zekios KC, Mouchtouri E-T, Lekkas P, Nikas DN, Kolettis TM. Sympathetic activation and arrhythmogenesis after myocardial infarction: where do we stand? J Cardiovasc Dev Dis 2021;8(5):57.
[22] Clemson PT, Hoag JB, Cooke WH, Eckberg DL, Stefanovska A. Beyond the baroreflex: a new measure of autonomic regulation based on the time-frequency assessment of variability, phase coherence and couplings. Front Netw Physiol 2022;2:891604.
[23] Cohen MA TJ. Short-term cardiovascular oscillations in man: measuring and modelling the physiologies. J Physiol 2002;542(Pt 3):669–83.
[24] Crampin E, Halstead M, Hunter P, Nielsen P, Noble D, Smith N, et al. Computational physiology and the physiome project. Exp Physiol 2004;89:1–26. https://doi.org/10.1113/expphysiol.2003.026740
[25] Bashan A, Bartsch RP, Kantelhardt JW, Havlin S, Ivanov PC. Network physiology reveals relations between network topology and physiological function. Nat Commun 2012;3:702.
[26] Task Force of the European Society of Cardiology and the North American Society of Pacing and Electrophysiology. Heart rate variability: standards of measurement, physiological interpretation, and clinical use. Circulation 1996;93(5):1043–65.
[27] Valente M, Javorka M, Porta A, Bari V, Krohova J, Czippelova B, et al. Univariate and multivariate conditional entropy measures for the characterization of short-term cardiovascular complexity under physiological stress. Physiol Meas 2018;39(1):014002.
[28] Nollo G, Faes L, Porta A, Antolini R, Ravelli F. Exploring directionality in spontaneous heart period and systolic pressure variability interactions in humans: implications in the evaluation of baroreflex gain. Am J Physiol-Heart Circ Physiol 2005;288(4):H1777–H1785.
[29] Pernice R, Sparacino L, Nollo G, Stivala S, Busacca A, Faes L. Comparison of frequency domain measures based on spectral decomposition for spontaneous baroreflex sensitivity assessment after acute myocardial infarction. Biomed Signal Process Control 2021;68:102680.
[30] Pichot V, Corbier C, Chouchou F. The contribution of granger causality analysis to our understanding of cardiovascular homeostasis: from cardiovascular and respiratory interactions to central autonomic network control. Front Netw Physiol 2024;4:1315316.
[31] Faes L, Masè M, Nollo G, Chon KH, Florian JP. Measuring postural-related changes of spontaneous baroreflex sensitivity after repeated long-duration diving: frequency domain approaches. Auton Neurosci 2013;178(1):96–102.
[32] Faes L, Gómez-Extremera M, Pernice R, Carpena P, Nollo G, Porta A, et al. Comparison of methods for the assessment of nonlinearity in short-term heart rate variability under different physiopathological states. Chaos Interdiscip J Nonlinear Sci 2019;29(12):123114.
[33] Barà C, Sparacino L, Pernice R, Antonacci Y, Porta A, Kugiumtzis D, et al. Comparison of discretization strategies for the model-free information-theoretic assessment of short-term physiological interactions. Chaos Interdiscip J Nonlinear Sci 2023;33(3):033127.
[34] Pinto H, Lazic I, Antonacci Y, Pernice R, Gu D, Barà C, et al. Testing dynamic correlations and nonlinearity in bivariate time series through information measures and surrogate data analysis. Front Netw Physiol 2024;4:1385421.
[35] Duncan TE. On the calculation of mutual information. SIAM J Appl Math 1970;19(1):215–20.
[36] Barrett AB, Seth AK. Practical measures of integrated information for time-series data. PLoS Comput Biol 2011;7:e1001052.
[37] Ay N. Information geometry on complexity and stochastic interaction. Entropy 2015;17(4):2432–58.
[38] Baptista MS, Kurths J. Transmission of information in active networks. Phys Rev E 2008;77:026205.
[39] Mijatovic G, Antonacci Y, Loncar-Turukalo T, Minati L, Faes L. An information-theoretic framework to measure the dynamic interaction between neural spike trains. IEEE Trans Biomed Eng 2021;68(12):3471–81.
[40] Faes L, Mijatovic G, Antonacci Y, Pernice R, Barà C, Sparacino L, et al. A new framework for the time- and frequency-domain assessment of high-order interactions in networks of random processes. IEEE Trans Signal Process 2022;70:5766–77.
[41] Schreiber T, Schmitz A. Surrogate time series. Phys D Nonlinear Phenom 2000;142(3):346–82.

[42] Faes L, Porta A. Conditional entropy-based evaluation of information dynamics in physiological systems. in: Wibral M, Vicente R, Lizier JT (Eds.), Directed Information Measures in Neuroscience, Springer Berlin Heidelberg, Berlin, Heidelberg, 2014, p. 61–86. https://doi.org/10.1007/978-3-642-54474-3_3
[43] Chicharro D. On the spectral formulation of granger causality. Biol Cybern 2011;105:331–47.
[44] Vicente R, Wibral M, Lindner M, Pipa G. Transfer entropy–a model-free measure of effective connectivity for the neurosciences. J Comput Neurosci 2011;30:45–67.
[45] Kozachenko LF, Leonenko NN. Sample estimate of the entropy of a random vector. Probl Peredachi Informatsii 1987;23:9–16.
[46] Kraskov A, Stögbauer H, Grassberger P. Estimating mutual information. Phys Rev E 2004;69:066138.
[47] Pinto H, Antonacci Y, Pernice R, Barà C, Javorka M, Faes L, et al. Decomposing the mutual information rate of heart period and respiration variability series to assess cardiorespiratory interactions. In: 2023 45th Annual international conference of the IEEE engineering in medicine & biology society (EMBC). 2023, p. 1–4.
[48] Prichard D, Theiler J. Generating surrogate data for time series with several simultaneously measured variables. Phys Rev Lett 1994;73:951–4.
[49] Schreiber T, Schmitz A. Improved surrogate data for nonlinearity tests. Phys Rev Lett 1996;77:635–8.
[50] Lancaster G, Iatsenko D, Pidde A, Ticcinelli V, Stefanovska A. Surrogate data for hypothesis testing of physical systems. Phys Rep 2018;748:1–60.
[51] Nollo G, Faes L, Porta A, Pellegrini B, Ravelli F, Del Greco M, et al. Evidence of unbalanced regulatory mechanism of heart rate and systolic pressure after acute myocardial infarction. Am J Physiol-Heart Circ Physiol 2002;283(3):H1200–H1207.
[52] Del Greco M, Nollo G, Disertori M, Sanna G, Maggioni AP. Non-invasive assessment of the arrhythmogenic substrate after myocardial infarction in the thrombolytic era: GISSI-3 arrhythmias substudy. G Ital Cardiol 1998;28:498–500.
[53] Nollo G, Del Greco M, Disertori M, Micciolo R, Maggioni AP, Santoro E, et al. Spectral and bidirectional filters give different results for signal-averaged ECG analysis in patients with postmyocardial infarction: GISSI-3 arrhythmias substudy investigators. J Electrocardiol 2000;33:233–40.
[54] Nollo G, Del Greco M, Disertori M, Santoro E, Maggioni AP, Sanna GP. Absence of slowest oscillations in short term heart rate variability of post-myocardial infarction patients. GISSI-3 arrhythmias substudy. GISSI-3 arrhythmias substudy investigators. Auton Neurosci 2001;90:127–31.
[55] Xiong W, Faes L, Ivanov PC. Entropy measures, entropy estimators, and their performance in quantifying complex dynamics: effects of artifacts, nonstationarity, and long-range correlations. Phys Rev E 2017;95:062114.
[56] Gibbons JD, Chakraborti S. Nonparametric statistical inference: revised and expanded. CRC Press; 2014.
[57] McDonald JH. Handbook of biological statistics. Baltimore: Sparky House Publishing; 2009.
[58] Sawilowsky SS. Real data analysis. IAP; 2007.
[59] Šidák Z. Rectangular confidence regions for the means of multivariate normal distributions. J Am Stat Assoc 1967;62:626–33.
[60] Pernice R, Volpes G, Cairo B, Gambardella M, Marchi E, Bassi AM, et al. Spectral decomposition of cerebrovascular and cardiovascular interactions in patients prone to postural syncope and healthy controls. Auton Neurosci 2022;242:103021.
[61] Barà C, Pernice R, Catania CA, Hilal M, Porta A, Humeau-Heurtier A, et al. Comparison of entropy rate measures for the evaluation of time series complexity: simulations and application to heart rate and respiratory variability. Biocybern Biomed Eng 2024;44(2):380–92.
[62] Bellman R. Dynamic programming. Science 1966;153(3731):34–7. https://doi.org/10.1126/science.153.3731.34
[63] Faes L, Nollo G, Porta A. Information domain approach to the investigation of cardiovascular, cardio-pulmonary, and vasculo-pulmonary causal couplings. Front Physiol 2011;2:80.
[64] Porta A, Castiglioni P, Rienzo MD, Bari V, Bassani T, Marchi A, et al. Short-term complexity indexes of heart period and systolic arterial pressure variabilities provide complementary information. J Appl Physiol 2012;113(12):1810–20.
[65] Kamiya A, Kawada T, Sugimachi M. Systems physiology of the baroreflex during orthostatic stress: from animals to humans. Front Physiol 2014;5:256.
[66] Faes L, Nollo G, Chon KH. Assessment of granger causality by nonlinear model identification: application to short-term cardiovascular variability. Ann Biomed Eng 2008;36(3):381–95.
[67] Mullen TJ, Appel ML, Mukkamala R, Mathias JM, Cohen RJ. System identification of closed-loop cardiovascular control: effects of posture and autonomic blockade. Am J Physiol-Heart Circ Physiol 1997;272(1):H448–H461.
[68] Takahashi A CM, Porta A, Melo RC, Quitério RJ, Silva Ed, Borghi-Silva A, et al. Aging reduces complexity of heart rate variability assessed by conditional entropy and symbolic analysis. Intern Emerg Med 2012;7(3):229–35.
[69] Lipsitz LA, Goldberger AL. Loss of 'complexity' and aging: potential applications of fractals and chaos theory to senescence. JAMA 1992;267(13):1806–9.
[70] Schmitt D, Stein P, Ivanov P. Stratification pattern of static and scale-invariant dynamic measures of heartbeat fluctuations across sleep stages in young and elderly. IEEE Trans Bio-med Eng 2009;56:1564–73. https://doi.org/10.1109/TBME.2009.2014819
[71] Ivanov P. Scale-invariant aspects of cardiac dynamics. Observing sleep stages and circadian phases. IEEE Eng Med Biol Mag Q Mag Eng Med Biol Soc 2007;26:33–7. https://doi.org/10.1109/MEMB.2007.907093
[72] Ivanov PC, Chen Z, Hu K, Eugene Stanley H. Multiscale aspects of cardiac control. Phys A Stat Mech Appl 2004;344(3):685–704. Proceedings of the International Workshop on 'Trends and perspectives in extensive and non-extensive statistical mechanics', in honor of the 60th birthday of Constantino Tsallis. https://doi.org/10.1016/j.physa.2004.08.016
[73] Dani M, Taraborrelli P, Panagopoulos D, Dirksen A, Torocastro M, Sutton R, et al. New horizons in the ageing autonomic nervous system: orthostatic hypotension and supine hypertension. Age Ageing 2022;51(8):afac150.
[74] Carrington CA, White MJ. Spontaneous baroreflex sensitivity in young and older people during voluntary and electrically evoked isometric exercise. Age Ageing 2002;31(5):359–64.
[75] Grieve DJ, Byrne JA, Cave AC, Shah AM. Role of oxidative stress in cardiac remodelling after myocardial infarction. Heart Lung Circ 2004;13(2):132–8.
[76] Jiang Y, Yabluchanskiy A, Deng J, Amil FA, Po SS, Dasari TW. The role of age-associated autonomic dysfunction in inflammation and endothelial dysfunction. GeroScience 2022;44(6):2655–70.
[77] Porta A, Baselli G, Guzzetti S, Pagani M, Malliani A, Cerutti S. Prediction of short cardiovascular variability signals based on conditional distribution. IEEE Trans Biomed Eng 2000;47(12):1555–64.
[78] Porta A, Guzzetti S, Furlan R, Gnecchi-Ruscone T, Montano N, Malliani A. Complexity and nonlinearity in short-term heart period variability: comparison of methods based on local nonlinear prediction. IEEE Trans Biomed Eng 2007;54(1):94–106.
[79] Bai Y, Siu KL, Ashraf S, Faes L, Nollo G, Chon KH. Nonlinear coupling is absent in acute myocardial patients but not healthy subjects. Am J Physiol-Heart Circ Physiol 2008;295(2):H578–H586.
[80] Zieman SJ, Melenovsky V, Kass DA. Mechanisms, pathophysiology, and therapy of arterial stiffness. Arterioscler Thromb Vasc Biol 2005;25(5):932–43.
[81] Huikuri HV, Seppanen T, Koistinen MJ, Airaksinen KEJ, Ikaheimo MJ, Castellanos A, et al. Abnormalities in beat-to-beat dynamics of heart rate before the spontaneous onset of life-threatening ventricular tachyarrhythmias in patients with prior myocardial infarction. Circulation 1996;93(10):1836–44.